ELSEVIER

Journal of Power Sources 81–82 (1999) 346–351

JOURNAL OF POWER SOURCES

www.elsevier.com/locate/jpowsour

The interaction between SnO anode and electrolytes

Jingze Li, Hong Li, Zhaoxiang Wang, Xuejie Huang, Liquan Chen *

Laboratory for Solid State Ionics, Institute of Physics, Chinese Academy of Sciences P.O. Box 603, Beijing 100080, China

Abstract

The electrochemical behaviors of nano-sized SnO anode in several electrolytes have been investigated. The SnO anode matched with 1 M $LiPF_6$ dissolved in ethylene cardonate/diethyl carbonate (EC/DEC) (1:1 v/v) shows the best performance. The discharge capacity at the 1st cycle reaches 1160 mA h/g. After 10 cycles, half of the initial capacity has been maintained. The cycling behaviors of SnO in other electrolytes, especially in PC based electrolytes, are rather poor. The FTIR results of SnO in PC and EC based electrolytes at discharged state confirmed that a passivating film composed of Li_2CO_3 and $ROCO_2Li$ is formed on the surface of SnO anode. It indicates that the cyclic performance of SnO anode is strongly influenced by the properties of the surface film.

Keywords: SnO anode; Electrolyte; Passivating film; FTIR; Cyclic voltammogram

1. Introduction

The successful utilization of carbonaceous materials as anode active material has led to the commercialization of Li-ion batteries [1]. However, the theoretical capacity of graphite is only 372 mA h/g. Recently, tin composite oxides (TCO) have been proposed as anode active material in lithium ion batteries [2–4]. They show larger reversible capacity more than 550 mA h/g. Tin-based oxide anode has entirely different reaction mechanism with lithium. Taking SnO as an example, lithium reacts irreversibly with SnO to form amorphous Li_2O and metallic Sn firstly, followed by a reversible alloying reaction with Sn [3–5]. We have already observed a shell structure on the surface of SnO particles at deep discharged state in 1 M $LiPF_6$, ethylene carbonate–diethyl carbonate (EC–DEC) (1:1) by HRTEM [5]. The shell is supposed to be a passivating layer and identified to consist of Li_2CO_3 and $ROCO_2Li$ using FTIR, which is similar to the case of carbonaceous anodes [6,7]. Based on FTIR results of SnO at different discharged states in 1 M $LiPF_6$ dissolved in EC–DEC (1:1 v/v), it has been confirmed further that Li_2CO_3 forms mainly above 0.9 V vs. Li/Li^+ and $ROCO_2Li$ forms below 0.7 V vs. Li/Li^+ [8].

It is well known that graphite is unstable in some aprotic electrolytes. For instance, when propylene carbonate (PC) is used as a solvent, the co-intercalation of solvent will lead to the exfoliation of graphite layers [9,10]. Only in selected electrolyte system, such as $LiPF_6$ in EC and DEC, graphite can present better cycling behavior. Therefore, a question may be raised naturally whether oxide anode is also sensitive to electrolyte or not. The purpose of this work is to study the behaviors of SnO electrode in several electrolytes using standard electrochemical techniques and FTIR.

2. Experimental

Nano-sized SnO powder was obtained by mechanical ball milling a commercial product for 8 h under an argon atmosphere using agate balls in the shearing mode. The weight ratio of balls to sample powder was 4:1. The image of TEM showed that the average size of SnO is around 100 nm [5].

Li/SnO cells were assembled in an argon-filled glove box. Working electrode is milled SnO with polyvinylidene difluoride (PVDF) as the binder (5% w/w) and carbon black as conductive additive (10% w/w), the counter-electrode is lithium foil. Celgard® 2400 microporous membrane is used as the separator.

All kinds of solvents, PC, dimethyoxy ethane (DME), dimethyl carbonate (DMC), DEC, EC, were purified by traditional method [11]. All electrolyte solutions, 1 M $LiClO_4$ in PC/DMC, 1 M $LiClO_4$ in PC/DME, 1 M

* Corresponding author. Tel.: +86-10-6258-2046; Fax: +86-10-6256-2605; E-mail: lqchen@aphy02.iphy.ac.cn

0378-7753/99/$ - see front matter
PII: S0378-7753(99)00263-3

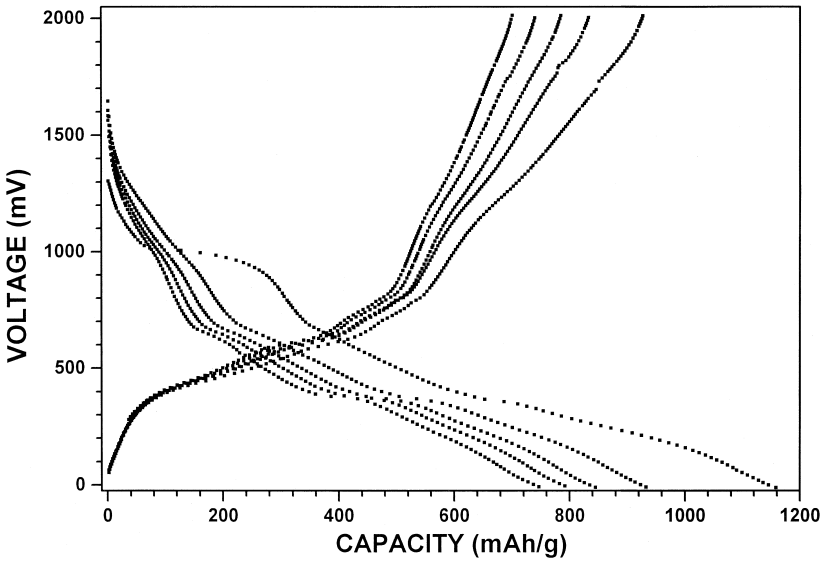

Fig. 1. Voltage profiles for the first five cycles of SnO anode in a cell: Li/1 M $LiPF_6$, EC–DEC (1:1 v/v)/SnO.

$LiClO_4$ in EC/DMC, 1 M $LiPF_6$ in EC/DEC (all 1:1 v/v), were purified before using.

The electrochemical cells were cycled at a constant current density of 0.2 mA/cm^2. The voltage window was limited between 0.0 V and 2.0 V. Cyclic voltammogram tests were carried out using CHI660A electrochemical workstation.

The electrodes for FTIR were prepared by directly pressing the milled SnO powder into pellets and dried at 80°C under vacuum for 24 h before assembling. Then, the assembled cells were discharged to 0.8 V at a constant current density of 0.1 mA/cm^2 and kept at this voltage for 48 h. After that, reacted SnO particles was ground together with KBr and pressed into pellets in the glove box. Finally, the pellets were sealed into a bottle in order to avoid the exposure during transferring process from globe box into the measured chamber of Bio-Rad FTS 6000 spectrometer.

3. Results and discussion

Fig. 1 shows the first five discharge/charge curves of SnO anode matched with 1 M $LiPF_6$ + EC/DEC. At the 1st discharge process, an irreversible voltage plateau at 1.0 V vs. Li/Li^+ is observed which is partly attributed to the reduction of the electrolyte and partly attributed to the

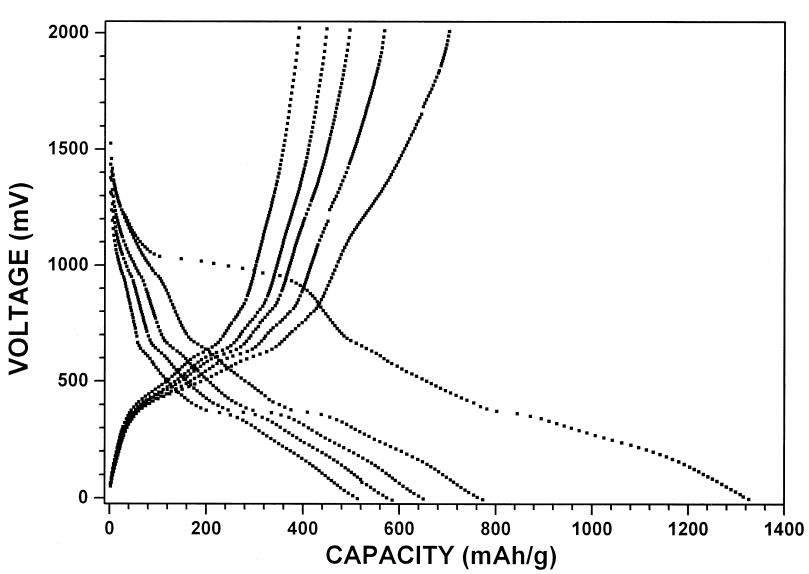

Fig. 2. Voltage profiles for the first five cycles of SnO anode in a cell: Li/1 M $LiClO_4$, PC–DMC (1:1 v/v)/SnO.

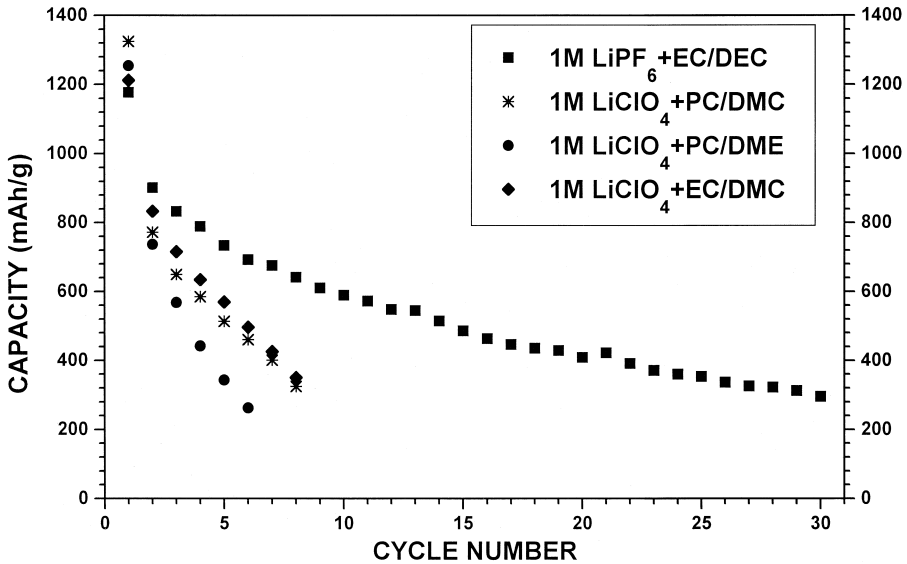

Fig. 3. Discharge capacity vs. cycle number of SnO anodes in several electrolytes.

replacement reaction of SnO [8]. The irreversible capacity loss corresponding to this plateau is about 220 mA h/g. The total discharge capacity at the 1st cycle is 1160 mA h/g. Concerning the theoretical capacity of SnO is 1270 mA h/g [3], small amount of SnO particles may not be reacted with lithium. In the following cycles, these unreacted SnO particles might take part in these reactions and contribute to the total capacity. At the 2nd discharge cycle, the irreversible plateau at 1.0 V becomes very small and gradually decreases with the cycle number. It should be pointed out that the capacity of $(n-1)$th $(n>1)$ charge process between 0.0 and 2.0 V is nearly equivalent to that of the nth discharge process. This indicates that the amount of extracted lithium can reversibly be inserted. In addition, the capacity between 0.8 and 2.0 V in charge process decreases significantly with the cycle number. It agrees with Dahn's opinion that the formation of metallic Sn above 0.8 V during the charge process may promote the aggregation process of Sn atoms; the aggregation will lead to the volume mismatch and the fracturing of active materials, resulting in capacity fade [12].

Fig. 2 displays the first five discharge/charge cycles of cell Li/$LiClO_4$, PC–DMC (1:1)/SnO in the same conditions as Fig. 1. The discharge profile at the 1st cycle is similar with that in Fig. 1. A plateau around 1.0 V is also observed. The capacity corresponding to the plateau is larger, about 300 mA h/g. The total capacity is as high as 1330 mA h/g. However, the charge capacity at the 1st cycle is smaller than that in Fig. 1. In addition, the discharge capacity decreases more quickly with cycling.

Fig. 3 represents typical cycle life behaviors during prolonged experiments of SnO electrodes in several electrolytes. The cell matched with 1 M $LiPF_6$ dissolved in EC/DEC showed the best cycling performance. At the 10th cycle, 50% of initial discharge capacity can be maintained. For other electrolytes, the cycling performance is rather poor.

The reversible and irreversible capacities of SnO anode for the 1st and the 5th cycle in four kinds of electrolytes are reported in Table 1. The irreversible capacity loss in electrolyte $LiPF_6$ + EC/DEC on the 1st and 5th cycle is much less than those in the other electrolytes.

The cyclic voltammograms of SnO electrode in two kinds of electrolyte $LiPF_6$ + EC/DEC and $LiClO_4$ + PC/DME were shown in Figs. 4 and 5, respectively. An irreversible reduction peak around 0.8 V vs. Li/Li^+ during the 1st cycle is observed in both figures. On the 2nd cycle, this peak weakens greatly. On the 3rd cycle, it almost disappears. Two significant differences can be found compared with these two figures. The peak current in Fig. 5 drops much faster than that in Fig. 4, which is consistent with the result of discharge/charge curves shown in Fig. 1. In addition, the oxidation peak current around 0.64 V is larger than that around 0.56 V vs. Li/Li^+ in Fig. 4; but

Table 1
The reversible and irreversible capacity of SnO anode at the 1st and the 5th cycle in four kinds of electrolytes

Electrocyte	The 1st cycle capacity (mA h/g)		The 5th cycle capacity (mA h/g)	
	Reversible	Irreversible	Reversible	Irreversible
$LiPF_6$ + EC/DEC	927	220	700	47
$LiClO_4$ + EC/DMC	826	486	489	65
$LiClO_4$ + PC/DME	741	514	264	80
$LiClO_4$ + PC/DMC	702	524	390	123

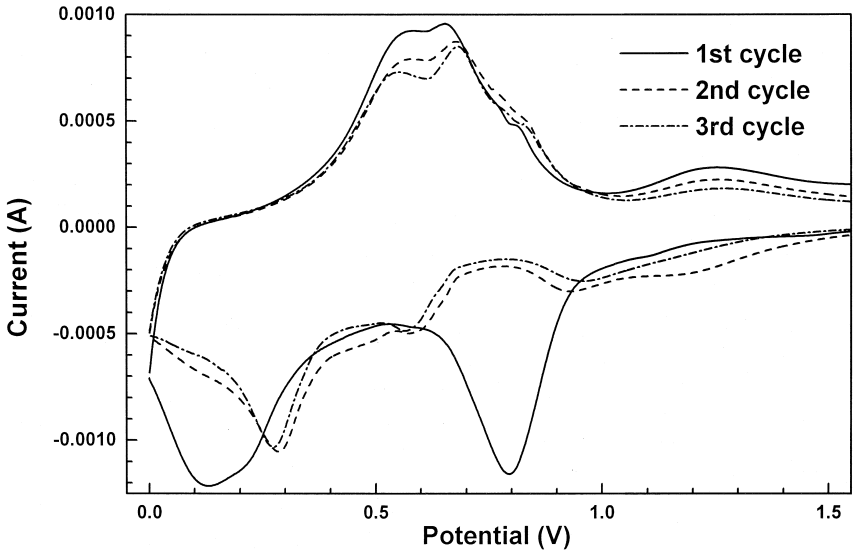

Fig. 4. Cyclic voltammogram of SnO electrode in 1 M $LiPF_6$, EC–DEC (1:1 v/v), scanning rate = 0.1 mV/s.

the opposite result is observed in Fig. 5. The reason is unknown. It might be related to the better capacity retention for SnO in $LiPF_6$ + EC/DEC.

Fig. 6 shows the IR spectrum of SnO anode discharged to 0.7 V in $LiPF_6$ + EC/DEC. Except the peaks related to residual EC, DEC and $LiPF_6$, the peaks at 1508, 1431 and 868 cm^{-1} are attributed to Li_2CO_3; the peaks at 1651, 1308 and 837 cm^{-1} are attributed to $ROCO_2Li$ [6,7,13–16].

The FTIR spectrum of SnO anode in $LiClO_4$ + PC/DMC after discharged to 0.8 V is shown in Fig. 7. The peaks at 1121, 1109, 1090, 629 cm^{-1} are attributed to $LiClO_4$ [13]. The peaks at 1630 and 1261 cm^{-1} belong to DME [14]. The peak at 1786 cm^{-1} is characteristic peak for PC [14]. Although a shoulder-peak presents at 849 cm^{-1} which is attributed to PC [14], the peak at 864 cm^{-1} related to Li_2CO_3 can be well recognized [13,15]. Other peaks corresponding to Li_2CO_3 (1433 cm^{-1} (νCO_3^{2-}), 1512 cm^{-1} (νCO_3^{2-})) are coupled with the bands of PC around 1443 and 1527 cm^{-1}. Due to strong peaks at 1630 and 1261 cm^{-1} for DME, 991 cm^{-1} for PC, it is difficult to determine the existence of lithium alkylcarbonates ($ROCO_2Li$) [14]. Anyway, Li_2CO_3 has already been identified to be main reduction products at 0.8 V vs. Li/Li^+ in

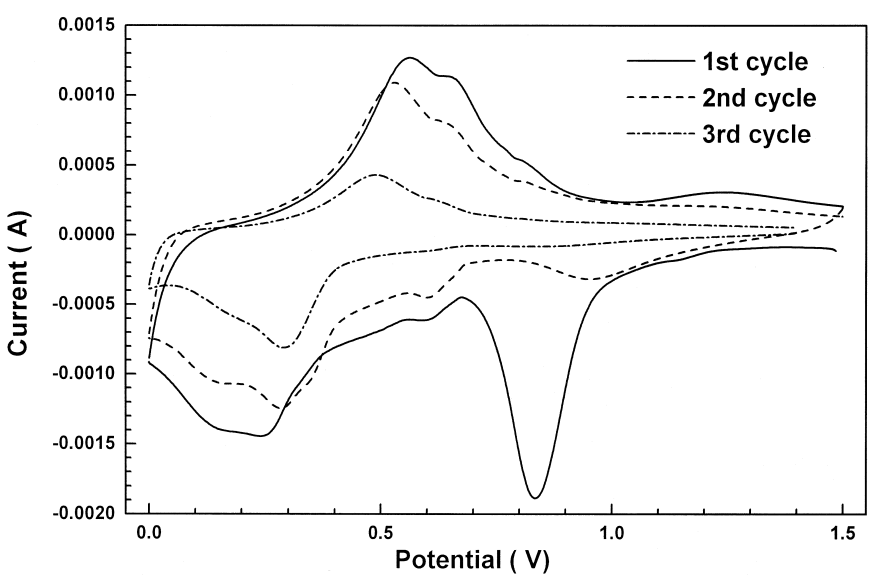

Fig. 5. Cyclic voltammogram of SnO electrode in 1 M $LiClO_4$, PC–DME (1:1 v/v), scanning rate = 0.1 mv/s.

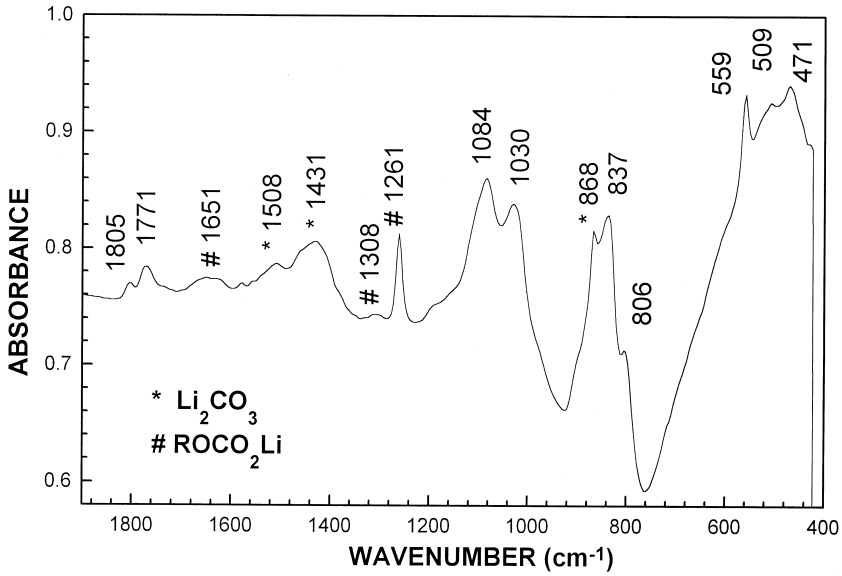

Fig. 6. FTIR spectrum obtained from reacted SnO after discharged to 0.7 V in Li/1 M $LiPF_6$, EC–DEC/SnO cell.

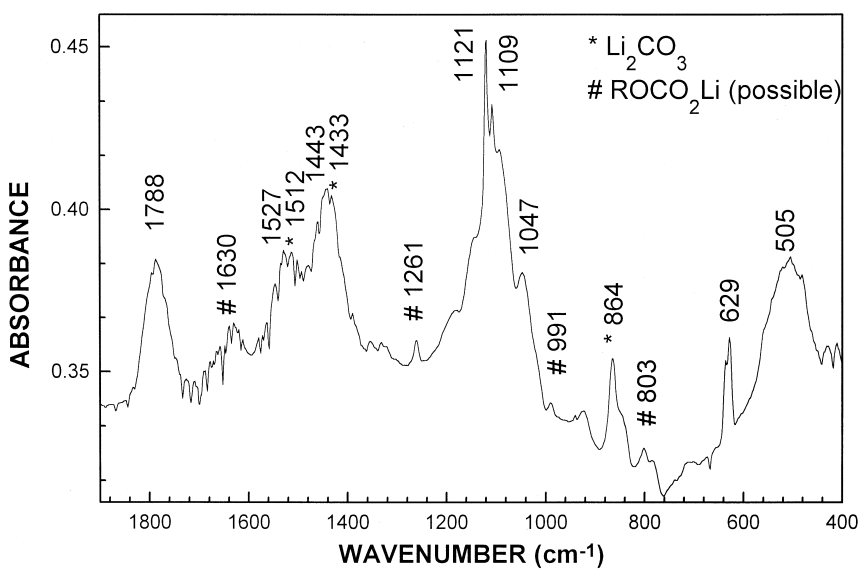

Fig. 7. FTIR spectrum obtained from reacted SnO after discharged to 0.8 V in Li/1 M $LiClO_4$ + PC/DME/SnO cell.

the 1st discharge process. It indicates that a passivating film was also formed on the surface of SnO anode in PC based electrolytes.

Since the co-intercalation of PC into oxide anode is not possible, it can be supposed that the electrochemical behavior of SnO anode depends strongly on the properties of the passivating film. Considering the electrochemical behaviors of SnO anode mentioned above, it could be supposed that in $LiPF_6$ + EC/DEC electrolyte, SEI on the surface of SnO may be well developed and kept stable with the cycles. While in other solutions, especially in PC based solutions, the SEI is less stable. Larger capacity loss of SnO anode in PC-based electrolyte at 1.0 V plateau (see Fig. 2) indicates that the surface film may be thicker than that in EC-bases electrolyte, which may increase the polarization of the electrode and reduce the utilization of active material. As a result, the capacity would fade rapidly with the cycle number.

4. Conclusions

The discharge/charge test of nano-sized SnO anode in several electrolytes confirms that the electrochemical behavior of SnO anode depends strongly on the composition of the electrolytes. The 1st discharge capacity of SnO in 1 M $LiPF_6$ + EC/DEC is around 1160 mA h/g. Reversible capacity of SnO is about 80% of the initial capacity on the 2nd discharge process. Until in the tenth discharge process, 50% of initial capacity can be maintained. While the

capacity retention upon cycling in other electrolytes, especially in PC based electrolytes, is rather poor. The sensitivity of SnO anode to electrolyte is related to the formation of a passivating film on the surface of SnO, which has been confirmed by FTIR analysis to SnO anodes in PC and EC-based electrolyte at discharged state.

Acknowledgements

This work was supported by Ford-NSFC Foundation (contract No. 9712304), NSFC (contract No. 59672027) and National 863 Key Program (contract No. 715-004-0280)

References

[1] T. Nagaura, K. Tazawa, Prog. Batteries Sol. Cells 9 (1990) 20.
[2] Y. Idota, T. Kubota, A. Matsufuji, Y. Maekawa, T. Miyasaka, Science 276 (1997) 1395.
[3] I.A. Courtney, J.R. Dahn, J. Electrochem. Soc. 144 (1997) 2045.
[4] W.F. Liu, X.J. Huang, Z.X. Xiang, H. Li, L.Q. Chen, J. Electrochem. Soc. 145 (1998) 59.
[5] H. Li, X.J. Huang, L.Q. Chen, Electrochem. Solid-State Lett. 1 (1998) 241.
[6] D. Aurbach, Y. Ein-Eli, B. Markovsky, A. Zaban, J. Electrochem. Soc. 142 (1995) 2882.
[7] A. Naji, J. Ghanbajia, B. Humbert, P. Willmann, D. Billaud, J. Power Sources 63 (1996) 33.
[8] H. Li, J.Z. Li, Z.X. Wang, X.J. Huang, L.Q. Chen, submitted to Electrochim. Acta.
[9] A.N. Dey, B.P. Sullivan, J. Electrochem. Soc. 117 (1970) 22.
[10] R. Fong, U. von sacken, J.R. Dahn, J. Electrochem. Soc. 137 (1990) 2009.
[11] J.T. Dudley, D.P. Wilkinson et al., J. Power Sources 35 (1991) 59.
[12] I.A. Courtney, J.R. Dahn, J. Electrochem. Soc. 144 (1997) 2943.
[13] R.A. Nyquist, R.O. Kagel, Infrared Spectra of Inorganic Compounds, Academic Press, 1971.
[14] D. Aurbach, M.L. Daroux, P. Faguy, E.B. Yeager, J. Electroanal. Chem. 297 (1991) 225.
[15] D. Aurbach, A. zaban, A. Schechter, Y. Ein-Eli, E. Zinigrad, B. Marhovshy, J. Electrochem. Soc. 142 (1995) 2873.
[16] D. Aurbach, A. Zaban, Y. Ein-Eli et al., J. Power Sources 68 (1997) 91.